

Werner Hufenbach¹, Maik Gude², Lothar Kroll³, Bernd Werdermann⁴, Andrzej Czulak⁵
 Technische Universität Dresden, Institut für Leichtbau und Kunststofftechnik (ILK), 01062 Dresden, Germany

MULTISTABLE FIBRE-REINFORCED COMPOSITES WITH CUTOUTS

During the manufacturing process and operating conditions of multilayered fibre-reinforced composites with variable fibre orientations, residual stresses build up due to the directional expansion of the unidirectionally reinforced single layers. Dependent on the laminate lay-up, these inhomogeneous residual stresses, which are primarily caused by thermal effects, moisture absorption and chemical shrinkage, can lead to large multistable out-of-plane deformations in the case of asymmetric laminates. For the calculation of the laminate deformations and the residual stresses especially around a notch, a dimensioning tool based on a modified stability analysis in combination with stress concentration model has been developed.

A solution method has been developed for stress concentration problems of fibre-reinforced compounds based on the method of complex-valued stress function combined with conformal mappings. Using this method, stress and displacement fields of anisotropic multilayered plates with cut-out can be calculated. For finite boundary the solution is analytically continued from the inner boundary to the rest of the plate. The remaining unknowns are obtained semi-analytically using a combination of boundary collocation method and least squares method. As the computation examples demonstrate, this analytical approach is markedly superior to a finite element analysis.

Key words: multistable composites, residual stresses, stress concentration

WIELOSTABILNE KOMPOZYTY Z WYCIĘCIAMI WZMOCNIONE WŁÓKNAMI

Podczas procesu produkcyjnego w kompozytach o zmiennej orientacji warstw powstają naprężenia własne w wyniku kierunkowego rozszerzenia się jednoosiowych warstw zbrojnych. Te niejednorodne naprężenia własne są głównie przyczyną efektów termicznych, absorpcji wilgoci i skurczu chemicznego. Mogą one w zależności od budowy laminatów prowadzić do dużych, wielostabilnych nieplaskich stanów odkształceń oraz generacji naprężeń własnych, zwłaszcza w okolicach karbu. Do rozwiązywania tych zagadnień stosuje się metody bazujące na zmodyfikowanej analizie stabilności w połączeniu z modelem naprężeń wokół karbu. Opracowana została metoda do analizy problemów związanych z koncentracją naprężeń we wzmacnianych włóknami komponentach, oparta na złożonych funkcjach naprężeń połączonych z odwzorowaniami konformalnymi.

Użycie tej metody pozwala na wyznaczenie wartości naprężeń i przemieszczeń wielowarstwowej płyty anizotropowej z wycięciem. Dla płyty o wymiarach skończonych można od granicy otworu analitycznie wyprowadzić warunki dla całej płyty. Wszystkie inne zmienne można uzyskać częściowo analitycznie, używając kombinacji metody kolokacyjnej oraz metody najmniejszych pierwiastków. Jak pokazano w przykładzie obliczonym numerycznie, zaprezentowane analityczne podejście pozwala uzyskać znacząco lepsze wyniki niż te wyznaczone przez metodę elementów skończonych.

Słowa kluczowe: kompozyty wielostabilne, naprężenia własne, spiętrzenie naprężeń

INTRODUCTION

In multilayered fibre-reinforced composites with variable fibre orientations, the directional expansion of the unidirectionally reinforced (UD) single layers due to thermal effects, moisture absorption and chemical shrinkage leads to a discontinuous residual stress field over the laminate thickness. In the case of asymmetric laminate plates, these residual stresses generally cause different multistable out-of-plane deformations. This paper focuses on the calculation of the deformation states and the arising residual stresses especially around a given notch.

Some earlier papers deal with the analytical calculation of the purely thermal out-of-plane deformations with the help of extended non-linear displacement-strain relations as well as by the Finite Element Analysis (e.g. [1-6]), however without taking advantage of the existence

of different stable equilibrium states for technical appli-

cations.

Basic ideas of technical applications of multistable laminates for adaptive structures were given in [7, 8]. Furthermore, the important influence of the chemical shrinkage and moisture absorption on the laminate deformation is not considered, although its contribution to residual stresses can be higher than the thermal contribution. Therefore the influence of shrinkage and moisture cannot be neglected in advanced design processes [8-11].

Considering extended stress-displacement relations, the principle of minimising the elastic potential in combination with the Rayleigh-Ritz method results in a system of non-linear equations for the calculation of the multistable laminate deformations. Dependent on the

¹ Prof. Dr.-Ing. habil., ^{2,3} Dr.-Ing., ⁴ Dipl.-Math., ⁵ Dipl.-Ing.

size and lay-up of the asymmetric laminate, the equation system leads to different solutions of stable, indifferent and unstable deformation states like saddle shapes or cylindrical shapes [2-5].

Additionally, a model for calculation of the stress concentration around given cutouts in multistable composites has been developed using complex-valued displacement functions and the method of conformal mapping.

The new laminate design method has successfully been verified by experiments and numerical calculations on asymmetric glass-(GFRP) and carbon-(CFRP)-fibre reinforced plastics and was successfully applied to the design of novel adaptive multistable composites with integrated smart alloys.

NON-LINEAR DEFORMATION THEORY OF UNSYMMETRIC COMPOSITES

For asymmetric laminates, the hygro-thermally and chemically caused directional deformations of the UD single layers result in large out-of-plane deformations. To take into account the large multistable deformations, which are often many times larger than the laminate thickness, the linear strain-displacement relations must be extended by non-linear terms (see e.g. [2, 3, 5, 8]):

$$\begin{aligned}\varepsilon_x &= \varepsilon_x^0 - z \frac{\partial^2 w}{\partial x^2} = \frac{\partial u^0}{\partial x} + \frac{1}{2} \left(\frac{\partial w}{\partial x} \right)^2 - z \frac{\partial^2 w}{\partial x^2} \\ \varepsilon_y &= \varepsilon_y^0 - z \frac{\partial^2 w}{\partial y^2} = \frac{\partial v^0}{\partial y} + \frac{1}{2} \left(\frac{\partial w}{\partial y} \right)^2 - z \frac{\partial^2 w}{\partial y^2} \\ \varepsilon_{xy} &= \varepsilon_{xy}^0 - z \frac{\partial^2 w}{\partial x \partial y} = \frac{1}{2} \left(\frac{\partial u^0}{\partial y} + \frac{\partial v^0}{\partial x} + \frac{\partial w}{\partial x} \frac{\partial w}{\partial y} \right) - z \frac{\partial^2 w}{\partial x \partial y}\end{aligned}\quad (1)$$

where the index 0 refers to the laminate reference plane.

The applied theory is based on the principle of minimising the total potential energy, which is given here by

$$\Pi = \int_V \left(\frac{1}{2} \bar{Q}_{ij} \varepsilon_i \varepsilon_j - \eta_{Ti} \varepsilon_i \Delta T - \eta_{Mi} \varepsilon_i \Delta M - \eta_{Si} \varepsilon_i \right) dV \quad (2)$$

with $(i, j = 1, 2, 6)$, where the \bar{Q}_{ij} are the reduced transformed stiffnesses, ΔT and ΔM are the differences in temperature and relative media concentration with respect to the reference state and η_{Ti} , η_{Mi} , η_{Si} are related to the elastic constants and to the thermal expansion coefficients α_j ($\eta_{Ti} = \bar{Q}_{ij} \alpha_j$), the swelling coefficients β_j ($\eta_{Mi} = \bar{Q}_{ij} \beta_j$) and the shrinkage s_j ($\eta_{Si} = \bar{Q}_{ij} s_j$), respectively [9].

Based on the total potential energy, the Rayleigh-Ritz method is applied to obtain approximate solutions

for the displacement fields. Therefore, general approaches in the form of polynomials are used dependent on the laminate lay-up.

For a square cross-ply $[0_n/90_n]$ laminate the occurring basic shapes are illustrated in Figure 1. Starting from the plane shape, which is considered as the reference state (Fig. 1a), the residual stresses lead to a saddle shape (b) or - dependent on the laminate dimensions and non-mechanical loads - to either of the two stable cylindrical shapes (c, d) (see also [2]). For $[0_n/90_m]$ laminates with $n \ll m$ or $n \gg m$ however only one stable cylindrical shape occurs.

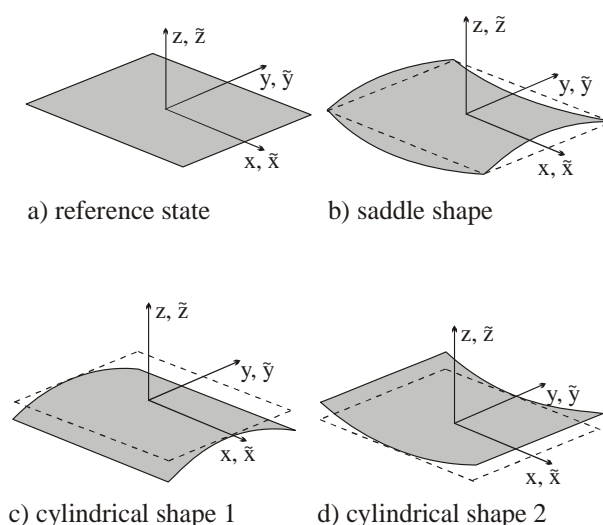


Fig. 1. Basic shapes of square $[0_n/90_n]$ laminates: a) reference state at elevated curing temperature, b)-d) saddle and cylinder shapes at room temperature

Geometrical assumptions for the out-of-plane displacements of cross-ply laminates lead to the general second order approach

$$w(x, y) = \frac{1}{2} (a_0 x^2 + b_0 y^2) \quad (3)$$

where the coefficients a_0 and b_0 define the laminate curvatures along the x and y axes [2-4]. For the description of the in-plane deformations, several approximations can be found in the literature [1, 3-5]. Based on geometrical assumptions, polynomials odd in x and even in y for $u^0(x, y)$ and polynomials even in x and odd in y for $v^0(x, y)$ are used. Further assumptions that ε_x^0 is independent on x , ε_y^0 is independent on y and the consideration of especially the non-linear terms in (1) reduce the amount of coefficients and finally lead to the approaches [8]:

$$u^0(x, y) = a_1 x - \frac{1}{6} a_0^2 x^3 + a_3 x y^2 \quad (4)$$

$$v^0(x, y) = b_1 y - \frac{1}{6} b_0^2 y^3 + b_3 y x^2$$

Using the displacement approximations (3) and (4) in the strain displacement relations (1) and substituting the resulting expressions into (2), the total potential energy of the laminate becomes a function dependent on the coefficients a_k, b_k ($k = 0, 1, 3$).

The principle of the minimum total potential energy requires the first variation to be zero, which means

$$\delta\Pi = \frac{\partial\Pi}{\partial a_k} \delta a_k + \frac{\partial\Pi}{\partial b_k} \delta b_k \equiv 0 \quad (5)$$

To satisfy this condition, every summand in (5) must be zero, which results in a coupled non-linear algebraic equation system in a_k, b_k . Dependent on the laminate lay-up and the laminate size, more than one solution can be obtained. These solutions have to be checked for their stability by means of $\delta^2\Pi$, which has to be positive definite for a stable deformation state.

ANALYSIS OF EXEMPLARY UNSYMMETRIC COMPOSITES

Applying the above mentioned theory, the solutions expressed in terms of the curvatures of an exemplary $[0_2/90_2]$ CFRP laminate are shown in Figure 2 dependent on the laminate edge length L . Branch AB shows the curvature of the stable saddle shape ($a_0 = -b_0$), which occurs in the case of small laminates. The critical edge length for the saddle shape is where the saddle shape becomes unstable, which defines the bifurcation point (B). Beyond this bifurcation point, the saddle shape occurs only theoretically as an unstable equilibrium state but not in reality, which is indicated by the dashed line BC. Instead of the stable saddle shape, now two equivalent stable solutions are calculated (BD and BE). Branch BD represents the curvature a_0 of the cylindrical shape in Figure 1d and the curvature $-b_0$ of the cylindrical shape in Figure 1c. Branch BE represents the secondary curvature $-b_0$ of the cylindrical shape in Figure 1d and the secondary curvature a_0 of the cylindrical shape in Figure 1c, which asymptotically approach zero with an increasing edge length L .

In Figure 3 the curvatures of GFRP and CFRP $[0_2/90_2]$ laminates cured at 125°C are compared dependent on the laminate's edge length. It can clearly be seen, that for this special stacking sequence the GFRP composite has a higher curvature than the CFRP laminate. However, several theoretical and experimental investigations on different asymmetric composites have shown, that a general statement about the comparison of curva-

ture magnitudes of laminates made of different materials cannot be made because of the significant influence of many different material parameters like $E_{\parallel}, E_{\perp}, \nu_{\parallel\perp}, G_{\parallel\perp}, \alpha_{\parallel}, \alpha_{\perp}$ and lay-up parameters like the number of layers, layer thickness and layer arrangement [8]. Instead, it has to be distinguished in each single case dependent on the lay-up, whether for example the GFRP or the CFRP laminate shows a higher curvature.

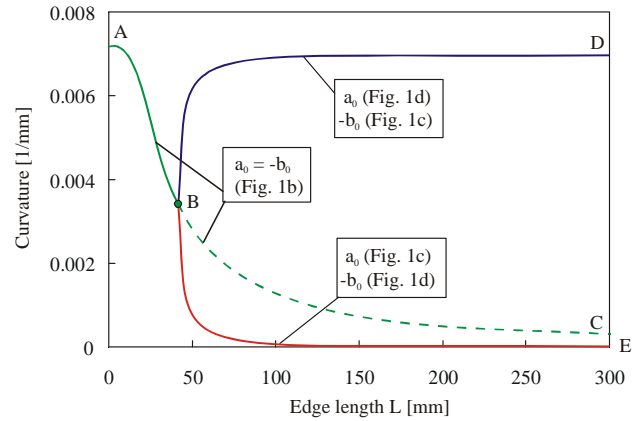


Fig. 2. Curvatures of a $[0_2/90_2]$ CFRP-laminate versus laminate edge length L

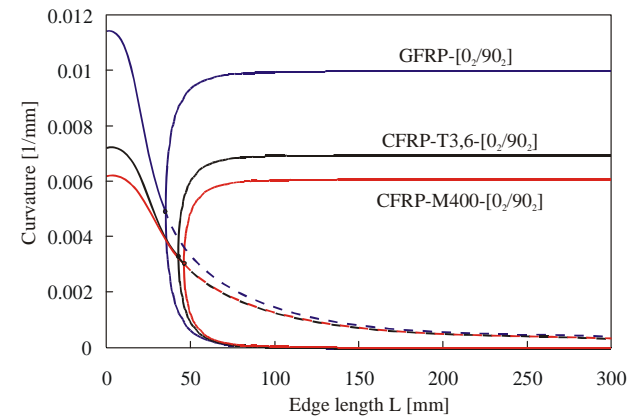


Fig. 3. Curvatures of different cross-ply laminates versus the laminate edge length L

STRESS CONCENTRATIONS AT HOLES

For the description of the stress concentration behaviour of multilayered composites, analytical calculation methods are developed at the Institut für Leichtbau und Kunststofftechnik (ILK). The model presented here is based on the enhanced laminate theory combined with the method of complex-valued displacement functions and the method of conformal mappings, from which adapted approaches for the stresses and displacements can be obtained. Especially, this model includes the uncommon coupling of membrane problems and plate bending problems, which occurs with unsymmetrical composites. E.g., Whitney [12] has demonstrated that

ignoring the membrane-bending coupling can lead to appreciable errors of up to 300% in this case.

Generalised plate equation

For a realistic stress concentration analysis of multi-layered composites, the composite is modelled as an infinite plate with a centric hole. Since such structures are thin-walled and the notch usually is small as compared to the overall dimensions of the structure, the vicinity of the hole is approximately plane and the structure can be locally described by means of the classical laminate theory. The following structural equation applies for the linear-elastic composite behaviour presupposed here:

$$\begin{pmatrix} N_x \\ N_y \\ N_{xy} \\ M_x \\ M_y \\ M_{xy} \end{pmatrix} + \begin{pmatrix} N_x^T \\ N_y^T \\ N_{xy}^T \\ M_x^T \\ M_y^T \\ M_{xy}^T \end{pmatrix} + \begin{pmatrix} N_x^Q \\ N_y^Q \\ N_{xy}^Q \\ M_x^Q \\ M_y^Q \\ M_{xy}^Q \end{pmatrix} = \begin{pmatrix} A_{11} & A_{12} & A_{16} & B_{11} & B_{12} & B_{16} \\ & A_{22} & A_{26} & & B_{22} & B_{26} \\ & & A_{66} & \text{symm.} & & B_{66} \\ \text{symm.} & & & D_{11} & D_{12} & D_{16} \\ & & & & D_{22} & D_{26} \\ & & & & & D_{66} \end{pmatrix} \begin{pmatrix} \varepsilon_x^0 \\ \varepsilon_y^0 \\ \gamma_{xy}^0 \\ \kappa_x \\ \kappa_y \\ \kappa_{xy} \end{pmatrix} \quad (6)$$

Here, N_i , M_i , N_i^T , M_i^T and N_i^Q , M_i^Q ($i = x, y, xy$) are the mechanically, thermally or media-induced stress resultants (forces or moments, respectively), which also lead to the global deformation of the structure as discussed in section 2. A_{ij} , B_{ij} , D_{ij} ($i, j = 1, 2, 6$) are the membrane, coupling and bending stiffnesses.

For consideration of the coupling effects of unsymmetrical composites, the Kirchhoff theory is expanded to the so-called Kirchhoff-Love theory by also including the normal stress resultants N_x , N_y , N_{xy} of the membrane problem into the equilibria of forces and of moments at the differential plate element $dV = dx \cdot dy \cdot h$, in addition to the bending loads (resultant moments M_x , M_y , M_{xy} , shear forces Q_x , Q_y , surface load $p(x, y)$):

$$\frac{\partial N_x}{\partial x} + \frac{\partial N_{xy}}{\partial y} = 0$$

$$\frac{\partial N_{xy}}{\partial x} + \frac{\partial N_y}{\partial y} = 0$$

$$\frac{\partial Q_x}{\partial x} + \frac{\partial Q_y}{\partial y} + p(x, y) = 0 \quad (7)$$

$$\frac{\partial M_x}{\partial x} + \frac{\partial M_{xy}}{\partial y} - Q_x = 0$$

$$\frac{\partial M_{xy}}{\partial x} + \frac{\partial M_y}{\partial y} - Q_y = 0$$

The structural law (6) as well as the strain-displacement relations for small deformations provide with (7) the generalised plate equation for composites, which comprises a coupling of the membrane and bending problems. If written as the vector equation suggested by Lepper [13]

$$\underline{\Delta} \begin{bmatrix} \underline{A} & \underline{B} \\ \underline{B} & \underline{D} \end{bmatrix} \underline{\Delta}^T \begin{bmatrix} u_0 \\ v_0 \\ w_0 \end{bmatrix} = -\underline{\Delta} \begin{bmatrix} N_T \\ M_T \end{bmatrix} - \underline{\Delta} \begin{bmatrix} N_Q \\ M_Q \end{bmatrix} + \underline{P} \quad (8)$$

it looks quite similar to the well-known Kirchhoff plate equation. Here, \underline{A} , \underline{B} , \underline{D} , \underline{N}_T , \underline{M}_T , \underline{N}_Q , \underline{M}_Q designate the respective matrices or vectors from (6), \underline{P} contains the surface $p(x, y)$ load (if present) and $\underline{\Delta}$ represents the matrix differential operator

$$\underline{\Delta} = \begin{bmatrix} -\frac{\partial}{\partial x} & 0 & -\frac{\partial}{\partial y} & 0 & 0 & 0 \\ 0 & -\frac{\partial}{\partial y} & -\frac{\partial}{\partial x} & 0 & 0 & 0 \\ 0 & 0 & 0 & \frac{\partial^2}{\partial x^2} & \frac{\partial^2}{\partial y^2} & 2\frac{\partial^2}{\partial x \partial y} \end{bmatrix} \quad (9)$$

The system of partial differential equations (8) can also be transformed into a single differential equation of the order eight in w_0 .

Complex-valued displacement functions and conformal mappings

The method of complex-valued stress or displacement functions, which is quite common in the theory of plane elasticity, is expanded here for solving the generalised plate equation using a displacement approach

$$w_0 = 2 \operatorname{Re} \left(\sum_{k=1}^4 \Psi_k(Z_k) \right) \quad (10)$$

with four analytical functions $\Psi_k(Z_k)$, which are related to four different complex planes $Z_k = x + \mu_k y$ ($k = 1 \dots 4$). To set up the boundary conditions for the stress

concentration problem, the notch area is reduced to the exterior of the unit circle through a conformal mapping, which is in general provided in series representation.

CALCULATION EXAMPLE

The evaluation of the developed analytical solution, including the determination of the terms of the series for the conformal mapping, can generally no longer be handled manually [13]. Therefore a computer programme has been created, which performs these calculations and presents the results in a graphic form. Thus, the programme enables rapid evaluation of the results and an efficient conduction of parameter studies.

As an example, the stress concentrations around a circular hole in the $[0_2/90_2]$ CFRP laminate discussed in section Analysis of exemplary unsymmetric composites have been calculated. Figure 4 depicts the tangential stresses around the hole at the surfaces of the 0° -layers as well as of the 90° -layers.

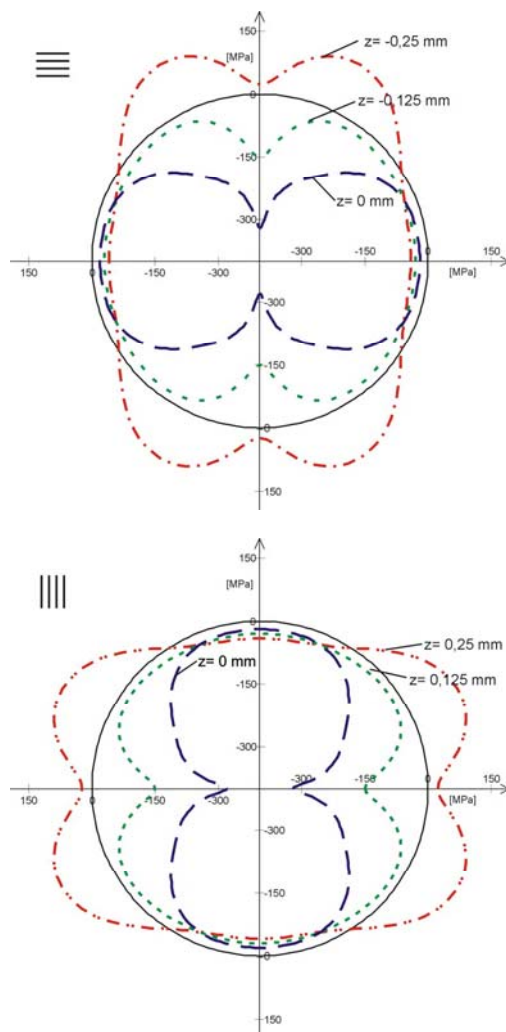


Fig. 4. Analytically-calculated tangential stress at a notch for a $[0_2/90_2]$ CFRP laminate (above: 0° layers, below: 90° layers)

CONCLUSIONS

The residual stress field, which builds up during the manufacturing process of multilayered fibre-reinforced composites with variable fibre orientations can be purposefully used to design asymmetric composites with defined deformation states and curvatures. Therefore, a modified stability analysis has been developed, which enables the prediction of the resulting monostable and

multistable deformation states due to thermal effects, moisture absorption and chemical shrinkage. The influence of cutouts on the residual stress field could be considered using a novel stress concentration model. It has been shown that the new calculation method enables a detailed assessment of the design parameters and serves for the efficient construction of multilayered composites with cutouts.

REFERENCES

- [1] Hyer M.W., Calculation of the Room-Temperature Shapes of Unsymmetric Laminates, *J. of Composite Materials* 1981, 15, 296-310.
- [2] Hyer M.W., The Room-Temperature Shapes of Four Layer Unsymmetric Cross-Ply Laminates, *J. of Composite Materials* 1982, 16, 318-340.
- [3] Jun W.J., Hong C.S., Effect of Residual Shear Strain on the Cured Shape of Unsymmetric Cross-Ply Thin Laminates, *Composite Science & Technology* 1990, 38, 55-67.
- [4] Peeters L.J.B., Powell P.C., Warnet L., Thermally-Induced Shapes of Unsymmetric Laminates, *J. of Composite Materials* 1996, 30, 603-626.
- [5] Dano M.-L., Hyer M.W., Thermally-induced deformation behavior of unsymmetric laminates, *Int. J. Solids and Structures* 1998, 35, 17, 2101-2120.
- [6] Schlecht M., Schulte K., Advanced calculations of the room-temperature shapes of unsymmetric laminates, *J. Composite Materials* 1999, 33, 16, 1472-1490.
- [7] Dano M.-L., Hyer M.W., Snap-through of unsymmetric fibre-reinforced composite laminates, *Int. J. Solids and Structures* 2002, 39, 175-198.
- [8] Gude M., Zum nichtlinearen Deformationsverhalten multistabiler Mehrschichtverbunde mit unsymmetrischem Strukturaufbau, Dissertation, TU Dresden 2000.
- [9] Hufenbach W., Kroll L., Gude M., Deformation States of Unsymmetric Fibre-Reinforced Composites Dependent on Residual Stresses, *Proc. of SAMPE EUROPE/JEC Conference, Paris 13.-15.04.1999*, 341-352.
- [10] Hufenbach W., Kroll L., Design and Construction of Hygro-Thermally Stable Shells, *Mechanics of Composite Materials* 1995, 31, 5, 677-683.
- [11] Hufenbach W., Gude M., Kroll L., Sokolowski A., Werdermann B., Adjustment of Residual Stresses in Unsymmetric Fibre-reinforced Composites Using Genetic Algorithms, *Mechanics of Composites Materials* 2001, 37, 1, 1119-130.
- [12] Whitney J.M., *Structural analysis of laminated anisotropic plates*, Technomic, Lancaster 1987.
- [13] Lepper M., *Kerbspannungsanalyse anisotroper Mehrschichtverbunde mit symmetrischem und unsymmetrischem*

Strukturaufbau, Dissertation, Technische Universität Claus-
thal 1999.

Recenzent
Jerzy Sobczak